The Journal of Transport and Land Use http://jtlu.org
Vol. 8 No. 3 [2015] pp. 115–129

Urban form and life-cycle energy consumption: Case studies at the city scale

Brice G. Nichols
Puget Sound Regional Council
bricenichols@gmail.com

Kara M. Kockelman
University of Texas at Austin
kkockelman@mail.texas.edu

Abstract: By combining daily (operations) and embodied energy demands, this work estimates life-cycle energy demands for residents and workers in different city settings. Using life-cycle analyses (LCAs) of different neighborhood types in Austin, Texas, this analysis fabricates five different city types, reflecting actual accessibility and resident and employment density profiles. Five residential and three commercial neighborhood types are distributed across 16-kilometer (10-mile) radius regions, with demographics held constant, for comparability. As expected, per-capita daily energy demands decrease with increased resident and employment density. Interestingly, embodied energy savings via increases in density are substantial. Though embodied energy makes up only 10-20 percent of total life-cycle energy, per-capita savings via density suggest it should be included in planning analyses. Overall, average life-cycle per-capita energy use ranges from 140 gigajoule (GJ)/year/capita in the least dense Orlando-style setting to around 90 GJ/year/capita in the maximum-density scenario, corresponding to a 35 percent reduction in per-capita energy demand. Energy reductions for Phoenix, Austin, and Seattle settings (relative to an Orlando-based design) are 18, 22, and 24 percent per-capita, respectively. Results provide a rare view of how total annual energy demands in both residential and commercial sectors are affected by density.

Keywords: Life-cycle energy analysis, built environment, urban form, transportation, land use, infrastructure

Article history:
Received: November 29, 2013
Received in revised form: July 27, 2014
Accepted: November 30, 2014
Available online: May 29, 2015

1 Introduction

Cities are facing unprecedented growth from rising population, migration, and urbanization. The United Nations (2011) anticipates global population to rise to 9.3 billion by 2050, by adding a net 2.3 billion new humans to the planet (a greater than 30 percent increase in population). Meanwhile, urban areas are projected to grow by 2.6 billion over the same time span. This suggests that over the next 35 years, cities will absorb all new population growth plus an influx from rural areas. From a global perspective, human populations are growing quickly, and urban areas are growing faster.

http://dx.doi.org/10.5198/jtlu.2015.598
ISSN: 1938-7849

The *Journal of Transport and Land Use* is the official journal of the World Society for Transport and Land Use (WSTLUR) and is published and sponsored by the University of Minnesota Center for Transportation Studies. This paper is also published with sponsorship from WSTLUR and the Institutes of Transportation Studies at the University of California, Davis, and the University of California, Berkeley.

These new residents, workers, and consumers will require more living and working spaces, and supporting infrastructure, and meeting those needs in an efficient way is often a challenge of planning, design, and political will. While much research has considered various aspects of how city form influences energy use and greenhouse gas emissions via transport behavior and building energy use, very little work actually aggregates the analysis to a larger city or regional scale. For instance, Cervero and Kockelman (1998) noted several built environment variables that influenced vehicle demand (and therefore energy consumption), but such findings have rarely been scaled up to consider how different urban forms compare in terms of total energy use as a function of these design variables. Newman and Kenworthy (1989) provided a well-known macro-level analysis of gasoline consumption in several different cities across the world, concluding that the built environment likely did have a large impact on gasoline consumption and automobile dependence, but their study emphasized a single energy-consuming sector.

Studies of the built environment's influences on consumption behavior (of vehicle kilometers, building energy, downstream noxious emissions, etc.) have generally been at a micro level, and have only included one or two parameters of the built environment. The result is a piecemeal image of how energy consumption varies across urban form, with little insight toward the "big picture" context of how urban planning influences energy usage at a city or regional level. For instance, in a meta-analysis of built environment factors, Ewing and Cervero (2010) suggest that land-use diversity had a weighted-average elasticity of around -0.09 with respect to vehicle-kilometers traveled (VKT), indicating that a doubling in land-use diversity tends to come with a 9 percent reduction in VKT. However useful such findings are, it is still unclear how a 9 percent reduction in driving really impacts a city in terms of relative energy use. When accommodating billions of new people, will land-use diversity really have as much of an impact on urban energy demand as building design, for instance?

Pivoting off the concept of relative energy demands by sector, recent research indicates that focusing even on all day-to-day energy demands ignores a rather important, but often ignored source of energy use: embodied energy used to construct, fabricate, ship, maintain, and eventually demolish and dispose of vehicles, buildings, and infrastructure components. Together, the day-to-day (operational) and embodied phases of specific materials or structures have been rather heavily researched (though much uncertainty surrounds the analyses) within the field of life-cycle analysis (LCA). LCA provides an appropriately holistic perspective on total energy (or greenhouse gas emissions) associated with many of the "building blocks" in the urban environment, but again, very few studies have attempted to aggregate the many micro-scaled LCAs to a city or regional level. Most studies focus on tracing energy pathways for distinct materials (e.g, Hammond and Jones 2008), or single structures like single-family homes (e.g., Keolian, Blanchard, and Reppe 2001), or various types of commercial buildings (e.g., Junnila, Horvath, and Guggemos 2006; Fay, Treolar, and Iyer-Raniga 2000). However, a study by Norman, Mac Lean, and Kennedy (2006) did provide one of the first LCA perspectives, at a neighborhood level, to compare low- and high-density neighborhoods in Toronto. Their work defined energy sources by sector and phase for the different neighborhoods and identified distinct energy demands across the neighborhoods. Importantly, they conclude that the vast majority of energy consumption is from daily building and transportation uses, which are influenced by both urban form and consumption behaviors.

Nichols and Kockelman (2014) greatly extended Norman, Mac Lean, and Kennedy's (2006) neighborhood-level LCA concept to compare energy use by sector and phase across four distinctive residential neighborhoods in Austin, Texas. After controlling for demographics, they measured and modeled life-cycle energy use by setting, noting clear efficiency gains from increased density. They also found that daily (operational) energy use and transport and building uses dominate total energy consumption patterns. They quantified the energy costs of different built environments and created an approach for anticipating energy savings across residential contexts. Such findings are useful for guiding local land-use and building policies and should be extended to anticipate the energy impacts of different urban forms at the citywide and regional scales.

This study extends the scale of Nichols and Kockelman's (2014) work, by moving from single neighborhoods to entire cities, and from residential-only settings to more realistic land-use patterns. The analysis incorporates "building blocks" from different disciplines, including travel choices, building energy use, infrastructure design, and LCA to construct larger neighborhoods and finally city patterns. A set of sub-models works together to create neighborhood groups arranged to reflect the form of chosen U.S. cities. Modeled energy use by source and phase are evaluated and compared to infer the built environment's impact on larger-scale energy demands.

Table 1: Models and data sources for neighborhood-level LCA (from Nichols and Kockelman 2014)

Sector	Household Consumption Source(s)	Operational Energy	Embodied Energy	Model/Estimation Source	Data Source(s)
Buildings	Electricity use	☑		OLS	RECS (2009) and CBECS (2003)
Buildings	Natural gas use	☑		OLS	RECS (2009) and CBECS (2003)
Buildings	Building materials		☑	GIS	City of Austin (2013)
Transportation	Personal vehicles' fuel use	☑		OLS, Poisson, MNL	NHTS (2009)
Transportation	Transit fuel use	☑		OLS	Austin Travel Survey
Transportation	Streets		☑	GIS	City of Austin (2013)
Transportation	Sidewalks		☑	GIS	City of Austin (2013)
Infrastructure	Water and wastewater		☑	GIS	City of Austin (2013)
Infrastructure	Water and wastewater use	☑		GIS	City of Austin (2013)
Infrastructure	Street lighting	☑		GIS	Google Earth

2 Method

Five neighborhood types are compared here, using five different residential and three commercial "cells" from Austin, Texas. Energy-related behaviors of households and firms are modeled via continuous- and discrete-response models. These eight neighborhood-level cells are then arranged to reflect population, employment, and accessibility of existing and hypothetical U.S. cities and regions (assuming a 10-mile radius). As noted earlier, estimates of the cell-level behaviors follow work by Nichols and Kockelman (2014), so many method details can be found in that study. Their work is extended here to include another residential setting, to create new commercial cells and examine energy use at the scale of multifaceted cities, rather than relatively homogenous neighborhoods.

2.1 Neighborhood cells

Nichols and Kockelman (2014) estimated household energy use for four distinctive residential neighborhoods in Austin, Texas. Those neighborhoods were selected to represent a range of densities and building types, from highly suburban to a dense urban core. They were analyzed using GIS to determine energy-relevant building and infrastructure characteristics—like building size by type, sidewalk and roadway areas, water and wastewater pipes, public lighting, parking structures, and driveways. Energy consumption then was estimated in terms of annual gasoline, electricity, and natural gas use via a set of ordinary least-squares (OLS), Poisson, and multinomial logit (MNL) regression equations. These regression models estimate daily (operational) energy demands, while embodied energy was estimated using measured building areas and types. A wide variety of data sources were used to calibrate the models, including the Residential and Commercial Buildings Energy Consumption Surveys (RECS 2009 and CBECS 2003), the National Household and Austin Travel Surveys (NHTS 2009 and ATS 2006), and various GIS data provided by the City of Austin (2013).

Population characteristics also have major impacts on energy use (e.g., Kockelman et al. 2008). Household demographics were controlled for and then made consistent across the competing neighborhoods by using a representative sample from Austin's Census-based Public Use Microdata Sample (PUMS). In other words, a single, typical (PUMS-based) cross-section of households was placed into each neighborhood, so that final energy demands varied only as a function of built environment features, like population and jobs densities, rather than demographics. This homogeneous cross-section of households reflected Austin variations in household sizes, number of workers, and three income categories, resulting in 39 different household types, scaled to each neighborhood's actual, current population. (For example, in a neighborhood of 1000 households, 80 are of two-member, two-worker, medium-income type.)

3 Residential and commercial cell characteristics

In Nichols and Kockelman's (2014) analysis, total energy was evaluated for only the residential areas of each neighborhood. This analysis extends their work by recognizing the commercial areas that clearly exist in three of these five neighborhoods, resulting in eight distinctive cell types. In this construct, residential energy use is measured per capita while commercial energy is measured per worker. To appropriately allocate shares of energy vested in the built environment, embodied energy is allocated to residential (r) and employment (e) sources for a neighborhood *i* as follows:

$$EE_{r,i} = x_{r,i} \times EE_{tot,i} \quad (1)$$

where $EE_{r,i}$ is embodied energy allocated to residential components, $EE_{tot,i}$ is total embodied energy, originally calculated by Nichols and Kockelman (2014) for each neighborhood *i*, and $x_{r,i}$ is the share of total floor area (base footprint plus estimated floor areas) used for residences. [1] Embodied energy allocated to employment ($EE_{e,i}$) is the remaining share, calculated as unity less $x_{r,i}$ times total embodied energy for zone i. This weighting allows more representative distribution of embodied energy shares from streets, sidewalks, water and wastewater pipes, parking garages, and surface parking facilities. Without this adjustment, neighborhood infrastructure designed to support large commercial buildings will appear incorrectly inefficient on a per-capita basis. Operations energy from commercial and office electricity and natural gas use is assigned exclusively on a gigajoule (GJ)/year/employee basis, and lighting and water use is segmented by residential or commercial-office.

[1] Total building areas are calculated for residential, commercial, and office uses only. Other buildings (e.g., parking garages, government buildings, schools, industrial) are not considered in this split.

3.1 Residential cells

Table 2 reports neighborhood attributes for the five neighborhood types, as produced by Nichols and Kockelman (2014) and amended here with the fifth residential neighborhood—Austin's downtown or central business district (CBD). The top portion describes site characteristics and the bottom portion relays average estimated vehicle ownership (by type), kilometers driven, and electricity and natural gas consumption per household.

From these site attributes and model estimates, Nichols and Kockelman (2014) estimated operational and embodied energy across transport, buildings, and infrastructure sectors, with results shown in Table 3, in terms of annual GJ consumed per capita. Summing operational and embodied energy for each neighborhood yields grand totals of 124.99, 116.60, 89.17, 68.38, and 58.45 GJ/year/capita for neighborhoods 1R-WL, 2R-AM, 3R-HP, 4R-RS, and 5R-DT, respectively. In this approach, both operation and embodied energy (and therefore total life-cycle energy) decreases with increasing density. The least dense neighborhood (1R-WL) uses nearly 2.8 times the lifecycle energy of the most-dense setting (5R-DT).

Table 2: Residential neighborhood cell parameters and model outputs from Nichols and Kockelman (2014), based on Austin, Texas, neighborhoods

		1R–Westlake (WL)	2R–Anderson Mill (AM)	3R–Hyde Park (HP)	4R– Riverside (RS)	5R–CBD
		Large-lot single family homes (SFH)	Newer, small SFH	Mixed SFH, multi-family home (MFH)	Low-rise MFH	Residential and commercial/ office towers
Site Attributes and Behavioral Estimates						
Total population (Census 2010)		4865	3394	4939	7728	5,512
Total employment		2478	313	1,019	763	86,892
Total area (km2)		13.1	1.7	2.2	1.3	2.9
Population density (residents/km2)		2492	15,923	14,797	44,765	12,580
Employment density (employees/km2)		1269	1261	3054	3937	198,345
% detached SFH		93%	92%	65%	8%	6%
% Building floor area commercial/office		0.0%	2.6%	18.6%	14.3%	80.5%
Kilometers from centroid to Austin CBD		7.2	21.6	4	3.7	0
Streets (centerline km/capita)		21.87	24.83	19.47	5.31	2.38
(Directional) Sidewalks (km/capita)		4.55	36.40	12.05	4.78	2.90
Transit stops per km2		0	0	70	47	194
Water and wastewater pipes (km/capita)		22.79	18.93	20.34	6.24	1.71
Avg. LDV VKT per HH per year		13,196	12,849	11,389	11,420	2,221
Behavioral Estimates/Outputs						
Avg. vehicles per HH		1.69	1.68	1.27	1.04	1.43
Vehicle-type shares	Passenger car	64%	63%	68%	68%	64%
	Van	12%	12%	11%	12%	11%
	SUV and CUV	18%	19%	17%	17%	17%
	Pickup truck	6%	6%	3%	4%	7%
Avg. LDV fuel economy (km/gal)		37.3	37.5	37.8	38.1	38.0
Avg. LDV fuel use (gal/year/HH)		849	832	584	473	260
Annual transit kilometers per HH		1519	756	641	1223	219
Avg. HH NG use (GJ/year)		97.9	91.6	74.9	66.9	73.6
Avg. HH electricity use (GJ/year)		26.9	24.8	21.8	22.0	21.8

Table 3: Energy estimates for residential neighborhoods from Nichols and Kockelman (2014)

GJ/year/capita											
		Operational Energy					Embodied Energy				
		1R-WL	2R-AM	3R -HP	4R –RS	5R-DT	1R-WL	2R-AM	3R –HP	4R-RS	5R-DT
Transport sources	LDV fuel use	48.25	45.43	36.58	25.18	6.89	--	--	--	--	--
	Transit fuel use	0.57	0.41	0.23	0.29	0.07	--	--	--	--	--
	Parking garages	--	--	--	--	--	0.00	0.00	0.06	0.00	0.01
	Surface parking	--	--	--	--	--	0.00	0.00	0.35	1.00	0.01
	Sidewalks	--	--	--	--	--	0.05	0.31	0.09	0.04	0.07
	Streets and roads	--	--	--	--	--	8.66	10.82	6.01	2.28	2.49
Building sources	Res. – SFH	51.24	47.79	39.73	34.89	39.23	13.97	9.63	3.86	0.23	0.06
	Res. – duplex						0.04	0.00	0.20	0.03	0.00
	Res. – apt.							1.01	1.08	3.57	0.86
Infrastructure sources	Freshwater	0.39	0.39	0.39	0.39	0.39	0.34	0.25	0.20	0.23	0.12
	Wastewater	0.15	0.15	0.15	0.15	0.15	0.14	0.12	0.14	0.03	0.16
	Lighting	0.40	0.29	0.10	0.07	1.12	--	--	--	--	--
Transport	Sub-total	48.82	45.84	36.81	25.47	13.78	8.71	11.13	6.51	3.32	2.58
Buildings	Sub-total	51.24	47.79	39.73	34.89	39.23	14.80	10.64	5.14	3.83	0.92
Infra.	Sub-total	0.94	0.83	0.64	0.61	1.66	0.48	0.37	0.34	0.26	0.28
Grand Total		**101.0**	**94.46**	**77.18**	**60.97**	**54.67**	**23.99**	**22.14**	**11.99**	**7.41**	**3.78**

3.2 Commercial neighborhoods

Two of the original five neighborhoods did not contain sufficient commercial development to create appropriate commercial neighborhoods. (These neighborhoods, 1R-WL and 2R-AM, are the least dense locations and are primarily comprised of single family homes). Table 4 shows the resulting annual operating and embodied energy per neighborhood on a per worker basis.

Table 4: Commercial neighborhood cell results from Nichols and Kockelman (2014)

GJ/year/worker							
		Operation			Embodied		
		1C-RS	2C-HP	3C –DT	1C-RS	2C-HP	3C –DT
Transport sources	Parking garages	--	--	--	0.00	0.03	0.00
	Surface parking	--	--	--	1.44	0.20	0.00
	Sidewalks	--	--	--	0.05	0.05	0.02
	Streets and roads	--	--	--	3.28	3.39	0.65
Building sources	Commercial	31.70	28.42	26.02	1.19	0.61	0.22
	Office					0.16	1.23
Infrastructure sources	Freshwater	0.48	0.18	0.02	0.32	0.11	0.03
	Wastewater	0.18	0.07	0.01	0.04	0.08	0.04
	Lighting	0.09	0.04	0.06	--	--	--
Transport	Sub-total	0.00	0.00	0.00	4.77	3.67	0.67
Buildings	Sub-total	31.70	28.42	26.02	1.19	0.77	0.45
Infrastructure	Sub-total	0.75	0.29	0.09	0.36	0.19	0.07
Grand total		**32.45**	**28.71**	**26.11**	**6.32**	**4.63**	**1.19**

Note that these neighborhoods are sorted from increasing employee density, which does not necessarily correspond to the ranking of residential neighborhoods, based off increasing population density. In this case, employment density of Hyde Park is higher than Riverside, even though the opposite is true of population density between the two neighborhoods. This analysis is based off methods and data previously collected by Nichols and Kockelman (2014). Results show that electricity and natural gas consumption for buildings is a major source of energy use, and greatly outweighs other sources from both operation and embodied phases. Overall, operation demands make up 84 to 96 percent of life-cycle energy demands for these neighborhoods, while buildings themselves make up 81 to 95 percent of total life-cycle energy demands. Annual life-cycle energy demands per worker are 38.7, 33.34, and 27.3 GJ for neighborhoods 1C-RS, 2C-HP, and 3C-DT, respectively.

4 City life-cycle energy model development

The set of five residential and three commercial settings can be combined in various ways to produce a life-cycle energy analysis at a larger, city-scale scope. Though much more variation occurs in reality, these eight neighborhood types represent a range of built environment types in a typical city—from sparse single-family home developments to more dense downtown environments and mixed styles in between. In the model, commercial and residential cells are overlaid and are independent of one another. For instance, a cell location may contain a high-density residential cell and a low-density commercial cell, or perhaps no employment or residential centers at all. In the synthetic cities, however, worker-resident ratios are held constant, and actual population and employment values were matched as closely as possible to maintain consistency.

4.1 City model structure

This city model considers a monocentric gridded cell city model, with square cell areas of 1.6 kilometers^2 (1 miles^2.) The model area contains a 16-kilometer (10-mile) radius from the city center, and a circular area described by the midpoint circle algorithm, for a total grid area of 798 kilometers^2 (308 miles^2.) The midpoint circle algorithm determines which cell centroids are within a given radius, so 1.6-kilometer (1-mile) distance bands can be created around the city center. Using this construct, two city forms are considered—one for residential neighborhood type distribution and the other for commercial neighborhoods. Energy (for operations vs. embodied, residential vs. commercial, transportation vs. infrastructure vs. buildings) is then tabulated for the city area, based on residential and commercial neighborhood attributes. Total population ($p_{i,j}$) and number of employees ($e_{i,j}$) per cell (with horizontal coordinate *i* and vertical coordinate *j*) is calculated as a function of underlying neighborhood population and employment densities (ρ_r and ρ_c, respectively) and cell area ($A_{i,j}$) as follows:

$$p_{i,j} = \rho_r A_{i,j} \tag{2}$$

$$e_{i,j} = \rho_c A_{i,j} \tag{3}$$

Of course, cell area is kept constant at 260 hectares (1 miles^2), so total number of residents and employees is therefore equal to population and employment density on a per-hectare basis.

In addition to population and employment density distributions over space, job accessibility for cell *i,j* ($ACC_{i,j}$) is also computed using a gravity-based index as follows:

$$ACC_{i,j} = \sum_{m,n} (e_{m,n} \times c_{m,n}{}^{v}) \tag{4}$$

Index *m,n* is used to differentiate locations of cells inside the summation (across the city grid) from the accessibility calculation result for cell *i,j*. Travel cost between cell *i,j* and indexed zone *m,n* is represented here by $c_{m,n}$. The *v* term is a scaling factor to model non-linearly decreasing accessibility as a function of travel cost. In this model, a scaling factor of -0.35 is selected based on calibration to San Francisco (Cervero, Rood, and Appleyard 1999). The accessibility model used here considers a very simple and linear travel cost function based on cell centroid distance between cells *x* and *y* as follows:

$$c_{m,n} = \sqrt{(x_{ij} - x_{mn})^2 + (y_{ij} - y^{mn})^2} + r \tag{5}$$

where r is half the cell width (or the radius of an inscribed circle within [i,j]) added to ensure cm,n always exceeds zero and returns a valid accessibility value, since zero cannot be raised by a negative exponential *v*. This value also represents the average distance traveled within a cell to reach a local destination within the same cell (i.e., on average, accessibility within a cell is not free of travel cost, and intra-cellular travel is assumed to be a function of the average distance of that cell). In this model, cell sizes are taken to be 1.6 kilometers^2 (1 mile^2) so r = 0.8 kilometer (0.5 mile).

4.2 Modeling case study cities

The intuitive city to model first is Austin, the city from which the neighborhoods were created. Four other cities are then also considered as model forms, including lower-density Orlando, Florida, and Phoenix, Arizona, and higher-density Seattle, Washington. New York City (NYC) was also considered, but Austin densities were simply never high enough to mimic the NYC reality. Nevertheless, this set of cities allows different urban forms to be explored and results compared across very distinctive US city settings. Moreover, a max-density case (a hypothetical city) was also developed. The method of recreating these five cities (four real and one hypothetical) using the eight Austin neighborhood cells is described below.

New-city creation was performed manually and rather intuitively, to best match existing neighborhood styles, as first viewed from satellite imagery, with the bank of eight cell types. The model cell sets were then updated/enhanced to more closely mimic the underlying actual population, employment density, and accessibility profiles of these five cities, as a function of distance to the regional/city centers. For instance, if Austin's population density within the first kilometer radius of the city center is 20,000 residents per kilometer, a set of neighborhoods was used to fill in the gridded cells to best reflect that density. The initial approach is subjective in terms of which exact cells are filled with specific neighborhood cell types to match satellite imagery, but density profiles then constrain the simulated patterns to much better reflect the true city's urban form.

Population and employment density, and accessibility profiles were calculated for Austin using data from the US Environmental Protection Agency's Smart Location Database (SLD) (see Ramsey and Bell 2013). The SLD is the only nationwide dataset that characterizes attributes like housing and employment density, as well as accessibility, land-use diversity, and transit coverage. SLD zones are based on Census block groups, and therefore vary in size depending on population density (Ramsey and Bell 2013). To calculate land-use metrics for Austin, distance bands were created, with 1.6-kilometer (1-mile) radius increments, beginning from a city center in Austin's CBD. The distance of each zone i,j from this city center was computed as follows:

$$d_{i,j} = \sqrt{(x_{i,j} - lat)^2 + (y_{i,j} - long)^2} \tag{6}$$

where $x_{i,j}$ and $y_{i,j}$ are latitude and longitude of the *i,j* zone's centroid, and *lat* and *long* are latitude and longitude of the city center. With this, cells were filtered for distance bands by selecting $d_{i,j}$ values within 1.6-kilometer (1-mile) ranges, out to 16 kilometers (10 miles).

The simulated city form was manipulated until each density and accessibility band reflected that of the city being modeled, such that actual city population and worker populations are within plus or minus 10 percent of one another, on average. Total city energy use was then calculated as the sum of the various different neighborhood types, assuming uniform energy demand profiles and populations for each neighborhood type. These models are thus somewhat rigid in their extension to city-level analysis, and probably should depend more on larger-scale city features, rather than on neighborhood-level details and a single, regional accessibility index. While the method could be improved by models more sensitive to other measures of the built environment (e.g., parking charges and local jobs-housing balance), this work provides a rare glimpse of energy consumption sources across various residential and commercial sources and phases in different settings, quickly and easily.

5 Results

The following results present the model and actual city density and accessibility profiles for the five case study cities (four real and one imagined) along with rather comprehensive LCA from resident and worker perspectives.

5.1 Synthetic city form

After matching cells with approximate land-use types, and adjusting cell placements to conform to actual-city density and accessibility metrics, five model cities were created. Figure 1 shows density profiles of the different city types considered

.

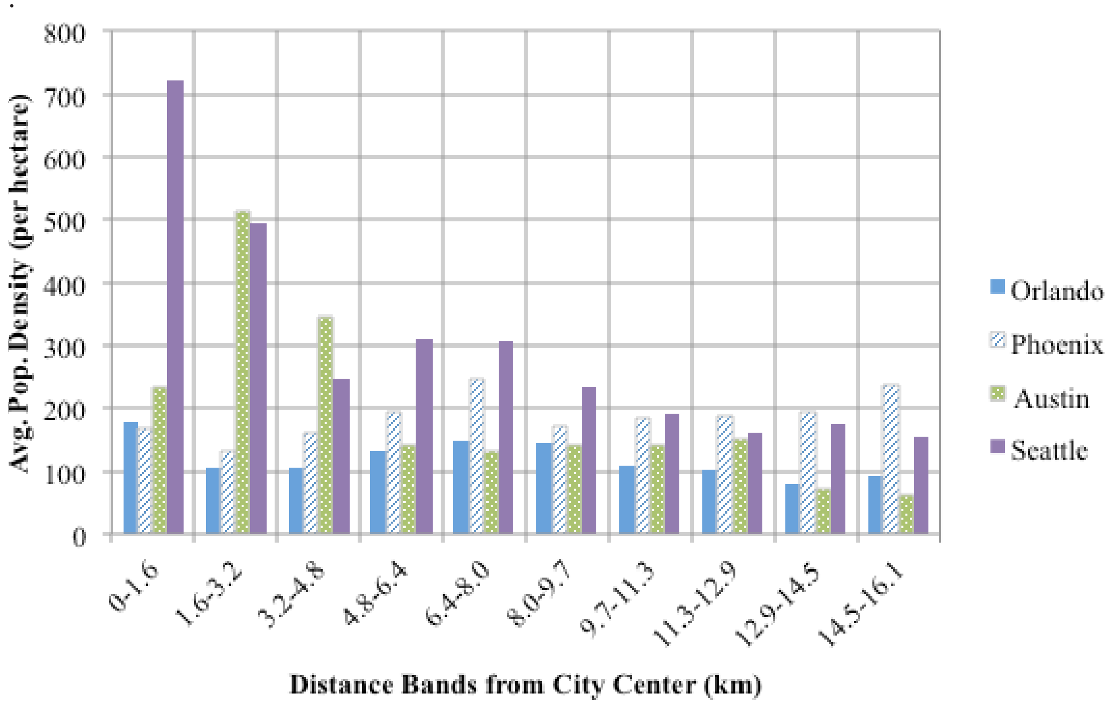

Figure 1: Comparing city population density profiles

Table 5 displays actual city parameters for average population and employment densities, resident-worker ratios, and life-cycle energy consumption estimates (from the model's many equations).

Table 5: Actual city parameters versus simulated city results

		Orlando, FL	Phoenix, AZ	Austin, TX	Seattle, WA	Max. Density Case
Real City Parameters						
Avg. population density (residents/hectare)		3.3	4.3	4.6	6.8	--
Avg. employment density (workers/hectare)		2.7	3.8	5.2	7.8	--
16.1-kilometer (10-mile) radius population		1,694,190	2,938,682	1,253,279	2,224,567	--
16.1-kilometer (10-mile) radius employment		934,052	1,640,268	679,658	1,245,834	--
Resident-to-worker ratio		1.81	1.79	1.84	1.79	--
Model Results						
Avg. population density (residents/hectare)		3.4	4.9	4.1	5.6	10.9
Avg. employment density (workers/hectare)		1.9	3.4	3.1	3.7	43.8
16.1-kilometer (10-mile) radius population		1,616,601	2,388,833	1,296,611	2,109,083	5,312,704
16.1-kilometer (10-mile) radius employment		816,576	1,663,494	686,003	1,219,742	4,756,135
Resident-to-worker ratio		1.88	1.44	1.9	1.73	1.12
City total (PJ/year)	Operations – res.	147.8	180.3	97.3	154.5	323.9
	Embodied – res.	48.8	43.1	22.4	34.0	39.1
	Operations – C/O	25.2	45.5	19.5	33.3	125.2
	Embodied – C/O	3.7	3.3	1.9	2.3	2.2
	Total operation	173.0	225.8	116.7	187.8	449.1
	Total embodied	52.5	46.4	24.3	36.3	41.3
	Life-cycle	225.5	272.2	141.0	224.1	490.3
City average (GJ/year/capita)	Operations – res.	91.5	75.5	75.0	73.3	61.0
	Embodied – res.	30.2	18.0	17.2	16.1	7.4
	Operations – C/O	15.6	19.1	15.0	15.8	23.6
	Embodied – C/O	2.3	1.4	1.5	1.1	0.4
	Total operation	107.1	94.5	90.0	89.1	84.5
	Total embodied	32.5	19.4	18.7	17.2	7.8
	Life-cycle	139.6	113.9	108.8	106.3	92.3
Operations (PJ/year)	Transport	71.0	82.1	44.5	70.3	135.3
	Buildings	100.3	141.7	71.1	115.9	310.0
	Other infra.	1.6	2.0	1.1	1.6	3.7
Embodied (PJ/year)	Transport	19.3	18.3	9.5	14.5	19.3
	Buildings	32.4	27.3	14.3	21.1	20.5
	Other infra.	0.7	0.9	0.5	0.7	1.4
Total (PJ/year)	Transport	90.3	100.3	54.0	84.7	154.6
	Buildings	132.7	169.0	85.4	137.0	330.6
	Other infra.	2.4	2.9	1.6	2.4	5.2

Figure 2 displays life-cycle energy demands across different city forms, separated by the energy use phase (embodied versus operational) and sector (transport versus building uses). Energy use phases include operational energy (OE), embodied energy (EE), and their total life-cycle energy (TOT).

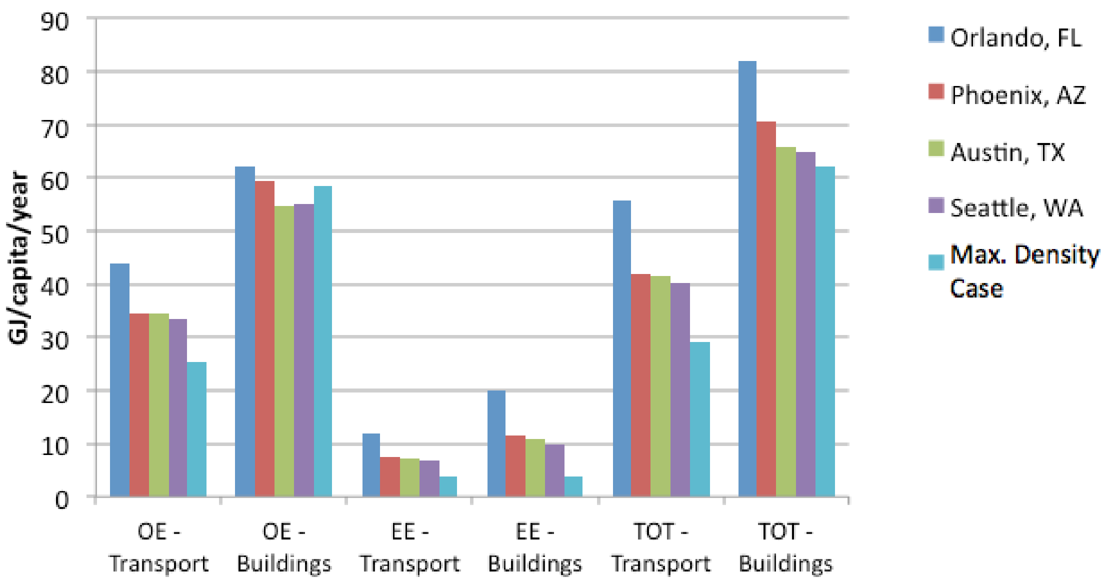

Figure 2: Energy consumption by city type, phase, and sector

6 Discussion

These model results provide a quantitative estimate of how city form influences per-capita energy-use rates at an aggregate level. These findings suggest that city form, measured by jobs accessibility, population, and employment density, are likely to affect per-capita energy consumption (and greenhouse gas emissions profiles, ceteris paribus). Additionally, such changes in energy use appear to emerge more readily from the embodied energy phase, as more residents and workers share existing infrastructure with greater intensity. Model results suggest that per-capita life-cycle energy in the maximum-density setting is only two-thirds that of the least dense (Orlando). While operational energy demands dominate total energy use, the most notable life-cycle energy savings, evident when shifting from the Orlando setting to a maximum-density (Austin-based) setting simulated here, come from the embodied energy phase. Per-capita embodied energy in the maximum-density setting is only one-quarter of that in Orlando. Operations energy, meanwhile, is about 20 percent less per person in this setting, versus Orlando. If one had higher-density cells to begin with, one could try to approximate plates like Chicago and New York, London and Beijing, and presumably arrive at even greater savings—especially in the embodied-energy domain. As the least dense and most energy-intensive environment for per-capita consumption, Orlando can be used as a pivot point to compare relative energy consumption across the four other city styles, as shown in Table 6.

Table 6: Per-capita annual energy savings, relative to Orlando setting

% Energy change (per capita) versus Orlando	Phoenix	Austin	Seattle	Max. density case
Operations phase	-11.8%	-16.0%	-16.8%	-21.1%
Embodied phase	-40.3%	-42.5%	-47.1%	-76.0%
Total life-cycle	-18.4%	-22.1%	-23.9%	-33.9%

These results indicate that built environment styles certainly vary across cityscapes, with efficiency increasing with density. This finding is clear in the operations phase, with efficiency increases between around 12 and 20 percent, but much more pronounced for embodied energy, with efficiency gains between 40 and 76 percent. Altogether, total life-cycle energy savings, when shifting from an Orlando-style setting, varies between around 20 and nearly 35 percent. This finding reinforces common perceptions that increasing resident and employment density reduces regional energy demand from day-to-day uses (i.e., the operations phase), but it also suggests that embodied energy savings contribute additional efficiency gains. By including this often "unseen" phase of energy consumption and considering a more holistic life-cycle perspective, density and accessibility become even more important metrics for improving regional energy efficiency, and consequently reducing greenhouse gas emissions and perhaps improving local air quality.

One challenge of this task is extrapolating a rather small set of selected Austin neighborhoods to higher-density environments. For instance, the maximum-density neighborhood of Austin (around 50 residents per hectare) is well below the average resident density of cities like New York and San Francisco. The maximum-density Austin neighborhoods fall well short of actual density profiles and so cannot represent all US or global city energy-use patterns. A more detailed analysis might extend the original neighborhood set to include more dense and diverse neighborhoods. As these neighborhoods are "building blocks," a standard set could be expanded for more detailed and finely tuned analyses.

7 Conclusions

This study provides rare insight into urban energy use on a large scale and includes a holistic perspective on energy use by sector and phase. It extends the concept of life-cycle analysis to a very aggregate level and then compares rather extreme city patterns in the United States. To the authors' knowledge, there are no other models that have attempted to quantify total life-cycle energy for a city at the scale of this work. Such results provide a context for evaluating the relative impact of energy savings schemes in various sectors and allow a more quantitative comparison of energy efficiency across different urban environments.

Results suggest that growing energy demands can be dampened, to some degree, by building cities with continued focus on infill and compact development, to promote density and reduce per capita life-cycle energy demands. Including a holistic perspective beyond the day-to-day energy demands allows one to quantify the efficiency gains of more intensively using public infrastructure and building stock, leading to less energy demand, fewer climate-altering emissions, and likely less cost. Density is often touted as a means to achieving efficiency, and this study bolsters that call by providing an additional dimension of analysis to understand energy demands more holistically. In many cases, when density is considered to reduce daily energy demands by a given amount, it is very likely that embodied energy savings would only amplify that value and bring even greater efficiency gains into the equation.

References

CBECS. 2003. Commercial Buildings Energy Consumption Survey. US Energy Information Administration, Washington DC.

http://www.eia.gov/consumption/commercial/data/2003/index.cfm?view=microdata.

Cervero, R., and K. Kockelman.1998. Travel demand and the 3Ds: Density, diversity, and design. *Transportation Research Part D* 2(3): 199–219.

Cervero, R., T. Rood, and B. Appleyard. 1999. Tracking accessibility: Employment and housing opportunities in the San Francisco Bay Area. *Environment and Planning* 31: 1259–1278.

City of Austin (2013) GIS Data. URL: ftp://ftp.ci.austin.tx.us/GIS-Data/Regional/coa_gis.html.

Ewing, R., and R. Cervero. 2010. Travel and the built environment. *Journal of the Architecture and Planning Association* 76(3): 265–294.

Fay, R., G. Treloar, and U. Iyer-Raniga. 2000. Life-cycle energy analysis of buildings: A case study. *Journal of Building Research and Information* 25(1): 31–41.

Hammond, G. P., and C. I. Jones. 2008. Embodied energy and carbon in construction materials. *Proceedings of the Institution of Civil Engineers: Energy* 161(2): 87–98.

Junnila, S., A. Horvath, and A. Guggemos. 2006. Life-cycle assessment of office buildings in Europe and the United States. *Journal of Infrastructure System* (12)1: 10–17.

Keolian G., P. Blanchard, and P. Reppe. 2001. Life cycle energy, costs and strategies for improving a single-family house. *Journal of Industrial Ecology* 4(2): 135–157.

Khan, M. 2000. The environmental impact of suburbanization. Journal of Policy Analysis and Management 19(4): 569–586. http://www.nbwctp.org/resources/the_environmental_impact_of_suburbanization.pdf.

Kockelman, K., M. Bomberg, M. Thompson, and C. Whitehead. 2008. *GHG Emissions Control Options: Opportunities for Conservation*. Washington, DC: National Academy of Sciences for the Committee for the Study on the Relationships Among Development Patterns, VMT, and Energy Conservation. http://www.caee.utexas.edu/prof/kockelman/public_html/NAS_CarbonReductions.pdf.

NHTS. 2009. Public Use Codebook, Version 2.1. National Household Travel Survey, Oak Ridge National Laboratory, U.S. Department of Transportation. http://nhts.ornl.gov/2009/pub/Codebook.pdf.

Newman, X., and X. Kenworthy. 1989. Gasoline consumption and cities: A comparison of US cities with a global survey. *Journal of the American Planning Association* 55(1): 24–37. URL: http://www.tandfonline.com/doi/abs/10.1080/01944368908975398#.U20hPvk8KSo.

Nichols, B., and K. Kockelman. 2014. Transportation systems and the built environment: A life-cycle energy case study and analysis. Submitted for presentation at the 93rd Annual Meeting of the Transportation Research Board, January 2013, and for publication in *Energy Policy*, August 2013. URL: http://www.caee.utexas.edu/prof/kockelman/public_html/TRB14neighborhoodsLCA.pdf.

Norman, J., H. Mac Lean, and C. Kennedy. 2006. Comparing high and low residential density: Life-cycle analysis of energy use and greenhouse gas emissions. *Journal of Urban Planning and Development* 132(1): 10–21. doi: 10.1061/(ASCE)0733-9488(2006)132:1(10).

Ramsey, K., and A. Bell. 2013. Smart Location Database. Version 2.0 User's Guide. Washington, DC: US Environmental Protection Agency. URL: https://edg.epa.gov/data/Public/OP/SLD/SLD_UserGuide.pdf.

RECS. 2009. *Residential Energy Consumption Survey*. Washington, DC: U.S. Energy Information Administration. URL: http://www.eia.gov/consumption/residential/data/2009/index.

cfm?view=microdata.

United Nations. 2011. *World Urbanization Prospects.* The 2011 Revision. Highlights. Washington, DC: Economic and Social Affairs, United Nations. URL: http://esa.un.org/unup/pdf/WUP2011_Highlights.pdf.